FINITE ELEMENT ANALYSIS OF PLASTICITY-INDUCED CRACK CLOSURE FOR INCLINED CRACKS

L.-W. Wei and M N James

Department of Mechanical and Marine Engineering, University of Plymouth, Drake Circus, Plymouth PL4 8AA, Devon, UK

ABSTRACT

This paper presents work on developing a finite element model to assess fatigue crack closure taking place in cracks which are inclined to the loading axis. Crack closure measurements were also performed on single-edge-notch tension (SENT) fatigue specimens made of an aluminium alloy Al5083-O, using the strain gauge based compliance method. It is found that cracks in SENT specimens are prone to changing growth direction from initial notches. Small variations in predicted crack opening level (S_{op}) were found for different inclinations to the specimen width direction, whereas predicted crack closing level (S_{cl}) demonstrated large change for the cases of $\alpha=45^0$ and 60^0. Reasonable agreement was obtained between the model results and the experimental data in cases of low mode ratio K_{II}/K_I ($\alpha=0^0$ and 15^0) which indicates (to some extent) the applicability of the numerical simulation of plasticity-induced crack closure for this class of inclined cracks.

1. INTRODUCTION

Since the discovery by Elber [1] of the phenomenon of premature contact between two crack faces in a growing fatigue crack, even under tension-tension loading, a large number of studies have been undertaken to estimate the magnitude of crack closure, and correlate it with crack growth behavior [2]. The kind of closure observed by Elber is often termed plasticity-induced closure, as it arises from contact, prior to the minimum cyclic load, of the residual plastically deformed material along the crack flanks behind the crack tip. The significance of understanding fatigue crack closure lies in the fact that it can not only provide some rationalization for certain anomalous behaviors such as the growth of physically short fatigue cracks and the stress ratio effect on growth rates, but also is required for more accurate life prediction. If the contributions due to crack closure are neglected, the driving force for crack growth, solely based on nominal loads, may differ between specimen and component, thereby leading to an erroneous life prediction.

The approaches to investigating plasticity-induced closure include experimental observations by means of various techniques such as the strain gauge based compliance method [1,3,4], analytical means evolved from the Dugdale strip-plasticity model [5,6], as well as numerical simulation using finite element analysis (FEA) [e.g. 7]. The pros and cons of these different methods have been critically reviewed by McClung and Sehitouglu [8]. In respect of FEA of plasticity-induced crack closure, efforts have been expended largely on two-dimensional FEA of fatigue crack closure assuming plane stress [7,8,9] or plane strain conditions [10,11], although some work has also been performed in a three-dimensional analysis of crack closure [12].

All this work on crack closure was, however, carried out on straight cracks which are situated either perpendicularly to the loading axis (pure Mode I) [e.g. **7,** 8], or parallel to it (pure Mode II) [13] or in a combination of the two previous cases (mixed Mode I and II loading) [9]. To the author's knowledge, there has been no finite element (FE) work which considered the closure behavior existing in cracks inclined to the loading axis, although this class of cracks is very commonly encountered in practice, e.g. crack deflection during growth. McClung & Sehitouglu [9] considered a case with mixed-mode loading, but their model can not be extended to the situation of crack deflection since the model only considered a symmetric system of both structure and loading. Suresh [14] developed a simple micromechanical model for crack closure due to crack path deflection, in terms of a combined geometric and linear elastic fracture mechanics analysis. In addition, Llorca [15] proposed a finite difference method to examine roughness-induced crack closure, which neglected plasticity-induced crack closure as well as the friction effect between crack faces.

The present work focuses its attention on FE modeling of plasticity-induced crack closure observed in edge cracks inclined at various angles, ranging from $\alpha = 0^0$ to $\alpha = 60^0$, to the specimen width direction. In contrast to the model developed by McClung & Sehitouglu [9], the model reported in this paper has the potential to incorporate crack deflection or roughness-induced closure with friction between surfaces being taken into account. For preliminary verification of the model, experimental determination of crack closure values was performed on single-edge-notch-tension (SENT) specimens of aluminum alloy Al5083-O with three different notch orientations ($\alpha = 0^0$, 15^0 and 60^0), using the strain gauge based compliance method. Analysis and discussion relevant to the FE modeling as well as to the experimental data are given in this paper.

2.   GENERAL PRINCIPLES OF FE MODELING OF FATIGUE CRACK CLOSURE

The establishment and evolution of the finite element method (FEM) has contributed greatly to the solution of many engineering problems, particularly in situations where analytical methods become too complex, and experimental techniques appear inappropriate because of either difficulties in application or instrumentation, or of the high costs which may be involved. One pronounced advantage of FEM lies in the fact that it can be used to solve a class of problems with only minor modifications once the model, boundary conditions, and accuracy have been tested and proven. The increasing computing power associated with faster processor speed and greater data storage capacity has also been a catalyst in developing FE applications. Hence, a great deal of work has attempted to solve the complicated issue of fatigue crack closure by means of FEM [e.g. 7].

In contrast to the simplicity of applying FEM to a static loading system, FE analysis of fatigue crack closure has been complicated by two features which accompany crack growth and closure under fatigue loading. These two features are crack extension and the flank contact behind the crack-tip. Representation of these two features in a FE model implies that the model must be able to accommodate both the change in boundaries and the likely contact of elements (i.e. new boundary conditions).

To handle crack extension in an FE model, several proposals have been put forward to release the crack-tip node. Some models have assumed crack extension at maximum load [7,10], some have allowed crack propagation at the minimum load of a cycle [16,17], and some even released the crack-tip node at an arbitrary point during a cyclic loading excursion [13]. Among these various crack-tip release proposals, the one proposed by Newman has been most often used, in which the crack-tip node is released at maximum load and the crack extended to the next node. More detailed discussions on node release schemes can be found in the work of McClung and Sehitoglu [8].

The nonlinear contact which occurs between the crack faces in the wake of the growing crack-tip has been treated in certain approaches [7,13,18]. Despite a few variations, the formulation proposed by Newman [7] has been generally used to treat the likely contact of crack faces. In Newman's method, two springs with varying stiffness are used to simulate contact and separation of the two crack faces. When the two crack faces make contact the stiffness of the springs is set to a substantially large value thus modeling a state of rigid contact, but when they separate the stiffness is set to zero, then simulating the condition of free opening between the crack faces. The implicit condition for this approach to be valid, is the existence of a plane of

symmetry between the two crack faces. The plane of symmetry can be taken as a rigid plane as no displacement at the direction normal to the plane is allowed for any point on the plane. Thus clearly the Newman's method cannot be used in the contact between crack faces of an inclined crack, due to the lack of symmetry along the crack plane in this case. The contact occurring in inclined cracks is a general contact problem, and thus a general contact analysis must be implemented in which a combined load and displacement control procedure is used. The commercial FE code Ansys 5.4 used in this work provides the utilities to deal with general contact problems.

3. MATERIAL, SPECIMEN AND EXPERIMENTAL TECHNIQUES

The material used in this work is an aluminium alloy Al5083-O. This material has gained a wide range of applications because of its moderate strength, weldability and good corrosion resistance [19]. Tensile testing was performed to obtain the monotonic and cyclic stress and strain curves, as shown in Figure 1. It can be seen from Figure 1 that the material shows cyclic hardening as do other aluminium-base alloys such as Al2024-T4 and Al7075-T6 [20]. The mechanical properties of this Al5083-O alloy are as follows; monotonic tensile yield stress, σ_y, of 145 MPa, initial cyclic tensile yield stress, σ_{oc}, of 240 MPa and Young's modulus (E) of 70GPa as well as a Poisson's ratio of 0.3. The cyclic stress-strain curve (Figure 1) was utilised in the FE analysis of fatigue crack closure. A Ramberg-Osgood relationship was used to fit the cyclic stress-strain curve which gives:

$$\frac{E\varepsilon}{\sigma_{0c}} = \frac{\sigma}{\sigma_{0c}} + 0.0757 \left(\frac{\sigma}{\sigma_{0c}} \right)^{15.17} \tag{1}$$

where σ and ε are stress and strain, respectively.

Closure data were obtained via a strain gage-based compliance technique. The digitally logged data were used to produce a differential stress-strain curve by subtracting the unloading linear portion from the original stress and strain data. The crack closure level is more readily identified from such an amplified change in slope of the differential stress-strain curve [21].

Surface strains were measured using small strain gauges with a gage length of 0.2 mm and a grid width of 1.4 mm. The gauges were located in the vicinity of the crack-tip with the gauge center being about 1 mm from the tip, and 0.5 mm above the crack line. This arrangement of strain gauges was suggested by Gan et al [3] as rather sensitive to the change in compliance due to the contact of crack faces. Data relevant to through-thickness closure were obtained from strain gauges placed on the back faces of 10 mm thick specimens.

SENT specimens of thickness 2 mm were used in the experimental testing with a maximum stress, S_{max}, of $0.85\sigma_y$ and a load ratio of R=0.05. This thickness gives, approximately, a state of plane stress in the specimen ($r_p/t \approx 1.25$), as simulated in the FE model. SET specimens 10 mm in thickness ($r_p/t \approx 0.25$) were also used with the aim examining crack closure levels under a stress state approximating plane strain. Initial notches 6 mm in length were machined in the samples along the rolling direction of the sheet from which the SET specimens were made, but with different inclinations to the specimen width direction. These angles included 0^0, 15^0, 30^0, 45^0 and 60^0, as shown in Figure 2. These different inclinations of notch provide different ratios of mixed-mode loading, provided that the fatigue crack propagates along the initial notch orientation (see Table 1). In practice, however, this initial plan was not successful for all the cases because of a change of growth direction from the initial notch orientation in cases with a medium or high value of mode-mixity, e.g. K_{II}/K_I =0.58 at α=30^0, K_{II}/K_I =1 at α=45^0 and K_{II}/K_I =1.73 at α=60^0, as shown in Table 1. Tanaka [22] performed fatigue tests using center-crack specimens which were prepared by growing a Mode I crack from a notch in a large specimen of pure aluminium, then cutting to the final shape with the initial crack being inclined at a certain angle to the specimen width direction. Using a constant load ratio R of 0.65 with different inclinations α of 0^0, 18^0, 45^0 and 60^0, Tanaka found that a crack would propagate along the

original crack direction if the equivalent stress intensity range (i.e. $\sqrt{K_I^2 + K_{II}^2}$) is above 1.6 times the equivalent threshold value of fatigue crack growth (i.e. $\sqrt{K_{I0}^2 + K_{II0}^2}$). His conclusion is not supported by the present work. The Mode I threshold value (ΔK_{I0}) for Al5083-O is about 5 MPa√m [23], and this is also the equivalent threshold value in the case of $\alpha=0^0$ due to absence of the Mode II component. It has been demonstrated by Tanaka [22] and Gao et al [24] that the equivalent threshold value under a pure Mode I condition (i.e. ΔK_{I0}) is greater than those for other Mode I and II combinations. The stress level used in the present work, $0.85\sigma_y$, produced an equivalent stress intensity range of 24 MPa√m for an inclination of $\alpha=0^0$ and 12 MPa√m for $\alpha=60^0$, all exceeding 1.6 times the Mode I threshold value of this material (i.e. about 8 MPa√m). However as indicated in Table 1, only in two cases (i.e. $K_{II}/K_I =0$ at $\alpha=0^0$ and $K_{II}/K_I =0.27$ at $\alpha=15^0$) did the cracks propagate along the initial notch orientation direction. The difference between the crack growth direction reported by Tanaka and that in the present work, may arise from the use of different types of specimen, different load ratios, or different precracking processes. As a result, experimental data for cases of higher Mode II component ($\alpha=30^0$, 45^0 and 60^0) can not be easily obtained with SENT specimens. However, the information on crack closure, obtained for the case of $\alpha=15^0$ (i.e. $K_{II}/K_I = 0.27$), is useful. The comparison between the predicted and experimental data, even restricted to the low angle case, still provides an indicator of the applicability of the model. In fact, it is likely that, if the contributions to closure due to the roughness of fracture surfaces are neglected, the underlying principle of crack deformation for all the cases of low and high Mode II components is essentially the same. In other word a FE model which is capable of modeling the case of low Mode II component, can theoretically be applied to other cases of higher Mode II components, in the absence of roughness effects.

4. FINITE ELEMENT MODELING

As discussed above, this work is primarily concerned with modeling the closure behavior of a crack, inclined to the loading axis in a SENT specimen made of Al5083-O, under constant amplitude fatigue loading and plane stress conditions. Kinematic hardening with the von Mises yield criterion, and the incremental plasticity flow law (the Prandtl-Reuss law) were utilised in the model. Constant amplitude fatigue loading was applied to the SENT model with a maximum stress, S_{max}, of $0.85\sigma_y$ and a load ratio of R=0.05.

The FE model is constructed using ANSYS 5.4, a commercial FE code package. Unlike the case of pure Mode I cracks in homogeneous materials which show symmetry along crack plane, cracks inclined to the tensile axis do not have such a feature. As a result, the whole structure of the specimen needs to be modeled. However, it should be pointed out that the modeling situation is more complicated than just a required meshing of the whole body. As mentioned before, it has been found by Tanaka [22] that depending on loading conditions, the crack may propagate either along the direction of the initial notch or change direction during subsequent growth to an angle to the initial notch orientation. In this preliminary study the case of a crack growing along its initial notch orientation has been investigated using FEM. The experimental data indicate that latter is even more significant in reality. The present model needs to be verified as producing reliable data before it is extended to cover the case of non-coplanar cracks arising from a shift of growth direction.

The initial notch length was taken as 6 mm, and the crack increment Δa (i.e. the smallest element size) was chosen as 0.125 mm following the suggestion made by McClung and Sehitoglu [8] where the relationship between crack increment (Δa) and plastic zone size is given by $\Delta a/r_p \leq 0.05$. This consideration is primarily based on the ability of the model to capture the local crack-tip deformation, and has nothing to do with actual crack growth rates. Clearly it is generally difficult for a numerical model to choose crack increments (the smallest mesh size) which correspond to the real growth rate due to the increase in computation time,

particularly in a PC based system as used in this work. However, as long as the model is fine enough to capture the plastic deformation near the crack tip, the size of crack increment should not greatly affect the closure levels [8]. The Newman crack-tip release scheme (i.e. the crack-tip extends one element length at the point of maximum load) was used in the FE model. Three-node plane stress elements were utilised in the model, together with surface-to surface contact elements to simulate the contact and separation of the two crack faces (Figure 3)

At the present time, no slipping friction between the two crack faces or crack deflection were considered in the model. Further work will attempt to incorporate these factors in the model, assisted by surface roughness maps which can be obtained from a scanning electron microscopy (SEM) package.

5. RESULTS AND DISCUSSIONS

Figures 4 and 5 present normalised model values of crack closure and crack opening (S_{cl}/S_{max} and S_{op}/S_{max}) respectively, versus the normalized crack length (a/W) for cracks at different angles of inclination to the specimen width direction. They also show the experimental data with mean values represented by dotted lines. Some observations can be made from these figures. First, the predicted crack closure values are generally larger than the corresponding opening values, which is qualitatively consistent with most of FE modeling work by other researchers [e.g. 7,25,26]. While there is negligible difference between S_{cl} and S_{op} in the case of $\alpha=60^0$ with both being about 30% S_{max}, the cases of $\alpha=0^0$ and 15^0 show differences between these two variables of up to 14%S_{max} (i.e. S_{cl} is some 43% greater than S_{op} for the cases of $\alpha=0^0$ and 15^0). Secondly, the opening values obtained for different angles of inclination are similar with a maximum difference of about 3% S_{max} between the cases of $\alpha=0^0$ and 45^0. However, the closure levels show appreciable variation (up to 13% S_{max}) with angle of inclination, except for the cases of $\alpha=0^0$ and 15^0. Thirdly, while generally the crack opening level S_{op} steadily increases to a stable value (between 27~33% S_{max} for all the angles of inclination), the crack closure values S_{cl} for the two large angles of inclination ($\alpha=45^0$ and 60^0) appear to maintain a steadily rising trend. This could be due to the fact that crack closure is highly sensitive to the residual deformation left in the crack-tip element and thereby to the mesh size, as was pointed out by Fleck [10]. It is also interesting to note that the S_{op} levels in the cases of two large inclinations ($\alpha=45^0$ and 60^0) are slightly higher than those for small inclinations ($\alpha=0^0$ and 15^0), whilst the reverse situations are found in the S_{cl} levels. This phenomenon is unusual as it is normally expected that a larger S_{cl} would lead to a larger S_{op} level. It is unclear at this moment whether these phenomena show inherent characteristics associated with closure behavior for inclined cracks, or whether they are artifacts introduced by the numerical procedure. Further work in refining the model, primarily in examining its sensitivity to mesh-size, and analysis of the displacement, stress and strain fields in the vicinity of the crack-tip, is needed to clarify the uncertainties.

The experimental work indicated that the S_{cl} values were similar to the S_{op} values, as listed in Table 2. The S_{cl} value obtained at the back face is lower than that obtained at near crack-tip locality for the 10 mm thick specimen, but the latter agrees well with the data determined from the specimen of thickness 2 mm (see No.2 and No.7 in Table 2). This is because the surface of the 10mm thick specimen approximates a state of plane stress, as in the 2mm thick specimen. On the other hand, the strain gauge at the back face of the 10 mm thick specimen reflects the plane strain state existing at the middle part of the specimen, which thus leads to a lower value of crack closure due to a less amount of residual plasticity left in the wake of the crack-tip.

Figures 4 and 5 indicate that S_{cl} values provide a better correlation between the model results and the experimental data (a maximum difference of around 10% S_{max} in the case of $\alpha=60^0$) than S_{op} values (a difference of up to 15% S_{max} in the case of $\alpha=0^0$). The difference may be attributed to many factors such as surface roughness or crack path deflection [14,27] which would inevitably contribute to the closure but which were not considered in the model. Incorporation of some of these factors in the model will be attempted in future work to provide a better estimate of crack closure levels. Despite these shortcomings, the

comparison between the model results and the experimental data is thought reasonable. This suggests that the FE model is capable of providing a useful estimate of crack closure values for inclined cracks, and warrants its extension to the case of non-coplanar cracks.

The data obtained experimentally for different nominal initial inclinations are similar, as shown in Table 2. This is due to the fact that crack propagation assumed similar directions in all the cases examined here, in spite of different initial notch orientations (see Table 1).

6. CONCLUSIONS

Based on the present work the following conclusions can be made.
1. A FE model was developed which can simulate plasticity-induced crack closure observed in cracks inclined to a loading axis. The applicability of the model has been tested through a comparison of the model results with the experimental data obtained in cases of low mode-mixity value (i.e. $K_{II}/K_I = 0$ and 0.27).
2. Small variations in predicted S_{op} (a difference of up to 3% S_{max}) were found for different inclinations to the specimen width direction, whereas predicted S_{cl} demonstrated large change (up to 13% S_{max}) for the cases of $\alpha=45^0$ and 60^0.
3. Cracks in SENT specimens are prone to grow in a direction which produces a maximum K_I.

ACKNOWLEDGMENTS

REFERENCES

1. Elber, W. (1970), *Engineering Fracture Mechanics* **2**, 37.

2. Newman, J.C. (1997), In: *Fatigue and Fracture Mechanics*, pp. 3-51. Underwood J.H., Macdonald, B.D. and Mitchell, M.R. (Eds), ASTM STP 1321.

3. Gan, D. and Weertman, J. (1981), *Engineering Fracture Mechanics* **15**, 87.

4. James, M.N. & Li, Wenfong (1997), *Materials Science and Engineering* **A265**, 129.

5. Budiansky, B. and Hutchinson, J.W. (1978), *J. of Applied Mechanics* 45, 267.

6. Newman, J.C. (1981), In: *Methods and Models for Predicting Fatigue Crack Growth under Random Loading*, pp. 53-84. Chang, J.B. and Hudson, C.M. (Eds), ASTM STP 748.

7. Newman, J.C. (1976), In: *Mechanics of Fatigue Crack Growth*, pp. 281-301, ASTM STP 590.

8. McClung, R.C. & Sehitouglu, H. (1989), *Engineering Fracture Mechanics*, **33**, 237.

9. McClung, R.C. & Sehitouglu, H. (1989), *Engineering Fracture Mechanics*, **33**, 253.

10. Fleck, N.A. (1986 *Engineering Fracture Mechanics*, **25**, 441.

11. Sehitoglu, H. & Sun, W. (1991), *J. Engineering Materials and Technology*, **113**, 31.

12. Chermahini, R.G., Shivakumar, K.N. and Jr, Newman, J.C. (1988) In: *Mechanics of Fatigue Crack Closure*, pp. 398-413, Newman, J.C., Jr. and Elber, W. (Eds). ASTM STP 982.

13. Nakagaki, M. & Atluri, S.N. (1980), *AIAA Journal*, **18**, 1110.

14. Suresh, S. (1985), *Metallurgical Transactions* **16A**, 249.

15. Llorca, J. (1992), *Fatigue Fract. Engng Mater. Struct.*, **15**, 655.

16. Ogura, K. and Ohji, K. (1977), *Engineering Fracture Mechanics* **9**, 471.

17. Nakamura, H. et al (1983), In: *Mechanical Behaviour of Materials (ICM 4)*, pp.817-823. Stockholm.

18. Blom, A.F. & Holm, D.K. (1985), *Engineering Fracture Mechanics* **22**, 997.

19. Davis, J.R. et al (1993), *Aluminium and Aluminium Alloys*. ASM International.

20. Suresh, S. (1991), *Fatigue of Materials*. The University Press, Cambridge.

21. Kikukawa, M., Jono, M and Tanaka, K. (1976), In: *Proceedings of the Second International Conference on Mechanical Engineering Material*, pp. 254-278. Boston, USA.

22. Tanaka, K. (1974), *Engineering Fracture Mechanics* **6**, 493.

23. Kaufman, J.G. & Kelsey, R.A. (1975), In: *Properties of Materials for Liquefied Natural Gas Tankage*, pp. 138-158. STP 579, ASTM.

24. Gao, H. et al (1985), In: *Multiaxial Fatigue*, pp. 184-202. ASTM STP 853.

25. Wu, J. & Ellyin, F. (1996), *Int. J. Fracture*, **82**, 43.

26. Ashbaugh, N.E. et al (1997), *Fatigue Fract. Engng Mater Struct* **20**, 963.

27. Ritchie, R.O. and Suresh, S. (1982), *Metallurgical Transactions* **13A**, 937.

TABLE 1

CRACK GROWTH DIRECTION RELATIVE TO NOTCH ORIENTATION

Specimen Number	Thickness (mm)	Notch angle (degree)	K_I (MPa m$^{1/2}$)	K_{II} (MPa m$^{1/2}$)	K_{II}/K_I	Crack growth direction relative to notch (degree)
1	2	0	24.00	0	0	0
2	2	15	21.82	5.85	0.27	0
3	2	30	17.54	10.13	0.58	+45.39 (side 1) +18.67 (side 2)
4	2	45	11.69	11.69	1	+24.50
5	2	60	5.85	10.13	1.73	+40.77
6	10	0	24.00	0	0	0
7	10	15	21.82	5.85	0.27	0
8	10	30	17.54	10.13	0.58	+30.56
9	10	45	11.69	11.69	1	+17.92
10	10	60	5.85	10.13	1.73	+34.88

Note: Crack growth direction is measured relative to notch orientation; the sign + denotes clockwise.

TABLE 2

EXPERIMENTAL DATA FOR S_{CL} AND S_{OP} VALUES

No.1 (t=2, $\alpha=0^0$)			No.2 (t=2, $\alpha=15^0$)			No.5 (t=2, $\alpha=60^0$)			No.7 (t=10, $\alpha=15^0$)		
a/W	S_{cl}/S_{max}	S_{op}/S_{max}	a/W	S_{cl}/S_{max}	S_{op}/S_{max}	a/W	S_{cl}/S_{max}	S_{op}/S_{max}	a/W	S_{cl}/S_{max}	S_{op}/S_{max}
0.2355	0.38	0.38	0.1969	0.40	0.40	0.3621	0.32	0.32	0.2532	0.32	0.32
0.2487	0.39	0.39	0.2124	0.43	0.43	0.41	0.43	0.43	0.2737	0.34 (0.26*)	0.34 (0.26*)
0.2684	0.51	0.51	0.2396	0.4	0.4	0.43	0.4	0.4	0.3023	0.43 (0.26*)	0.43 (0.26*)
0.3342	0.49	0.49	0.2669	0.47	0.47	0.4495	0.43	0.43	0.3105	0.53	0.53
0.3487	0.48	0.48	0.3145	0.43	0.43	0.5958	0.43	0.43			
			0.3281	0.45	0.45						
			0.3418	0.47	0.47						
Mean value	**0.45**	**0.45**		**0.436**	**0.436**		**0.402**	**0.402**		**0.405**	**0.405**

Note: * this value was determined from the strain gage in the back face of the specimen.
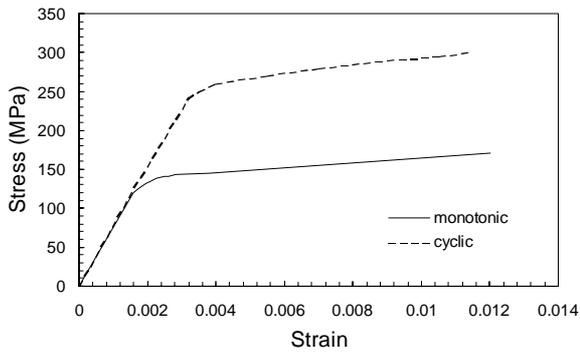
Figure 1: Monotonic tensile and cyclic stress-strain curves for Al5083-O.
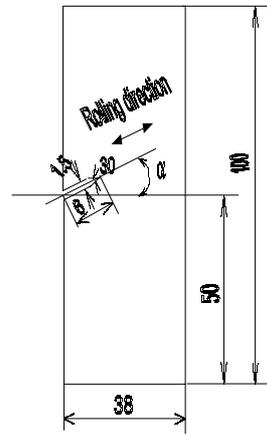
Figure 2: Schematic of the single-edge-notch-tension (SENT) specimen; $\alpha=0^0$, 15^0, 30^0, 45^0, 60^0.
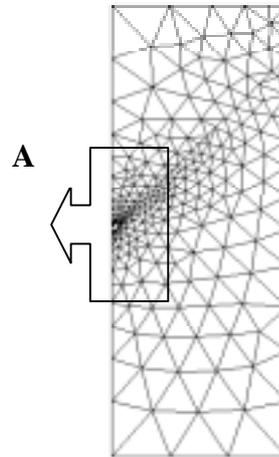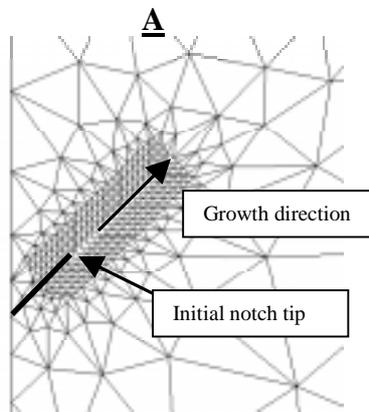
Figure 3: FE model for cracks propagating along the initial orientation; the left is the enlarged crack-tip region.
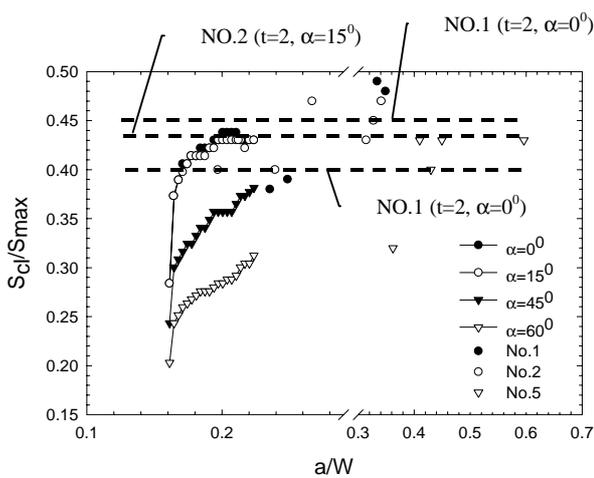
Figure 4: Comparison of the crack closure values determined from both the FE model and experiments. Dotted lines denote the mean experimental data.
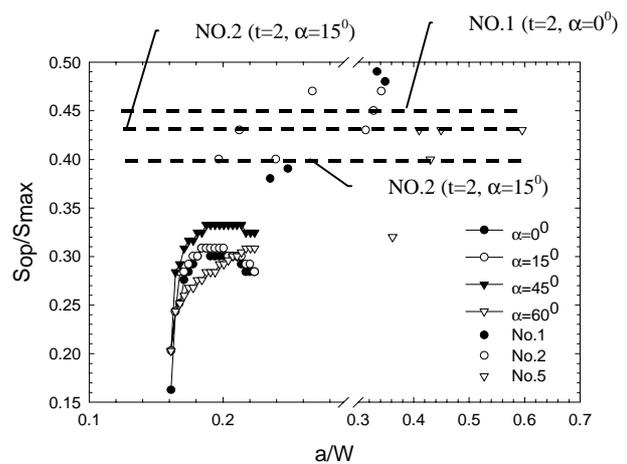
Figure 5: Comparison of the crack opening values determined from both the FE model and experiments. Dotted lines denote the mean experimental data.